A Non-Local Mode-I Cohesive Model for Ascending Thoracic Aorta Dissections (ATAD)

A non-local mode-I cohesive model for ascending thoracic aorta dissections (ATAD)

Gioacchino Alotta, Emanuela Bologna, Marzio Di Giuseppe, Massimiliano Zingales
University of Palermo
Palermo, Italy
gioacchino.alotta@unipa.it,
emanuela.bologna@unipa.it,
marzio.digiuseppe@unipa.it,
massiliano.zingales@unipa.it

Rossana Dimitri, Francesco Paolo Pinnola
University of Salento
Lecce, Italy
rossana.dimitri@unisalento.it,
francesco.pinnola@unisalento.it

Giorgio Zavarise
Politecnico di Torino
Torino, Italy
giorgio.zavarise@polito.it

***Abstract*—This paper presents a non-local interface mechanical model to describe aortic dissection. In this regard, the mode-I debonding problem based on a cohesive zone modeling is endowed with non-local terms to include long-range interactions that are present in multi-layered biological tissue. Such non-local effects are related to the collagen fibers that transmit forces between non-adjacent elements. Numerical simulations are provided with different values of the non-local parameters in order to show the effect of the non-locality during the debonding processes.**

Keywords—biomechanics; cohesive zone model; debonding process; non-local effects.

I. INTRODUCTION

Aortic dissection is not a common disease but it is highly lethal. The estimated incidence involves from 5 to 30 cases per million people per year. Population-based studies suggest that the incidence of acute dissection ranges from 2 to 3.5 cases per 100,000 person-years. It may occur that two to three times as many patients die of dissections as of ruptured aortic aneurysms; approximately 75% of patients with ruptured aortic aneurysm would reach an emergency department alive, whereas for aortic dissection 40% may die immediately. Furthermore, from 50% to 70% may be alive 5 years after surgery depending on age and underlying causes.

For an untreated acute dissection of the ascending aorta the mortality rate goes from 1% to 2% per hour after the onset. Type A dissections treated medically can occur within the first 24 hours (approximately 20% of them) or within the 1st month after presentation (approximately 50% of them). Even with surgical intervention, the mortality rate for type A dissection may be as high as 10% after 24 hours and nearly 20% 1 month after repair. Although type B dissection is less dangerous than type A, it is still associated with an extremely high mortality. The 30-day mortality rate for an uncomplicated type B dissection approaches almost a percentage of 10%. However, patients with type B dissection and possible complications such as limb ischemia, renal failure, or visceral ischemia have a 2-day mortality upwards of 20% and may prompt the need for surgical intervention.

Biomechanical models of interfaces are well known in the literature to represent a challenging step toward the prediction of the aortic dissection. In this regard, specific models in literature have never described interface and its debonding failure in mode-I condition, whereas biomechanical predictions have been only assessed with the aid of phenomenological failure criteria [1].

978-1-5386-6282-3/18/$31.00 ©2018 IEEE

In this work, the authors aim at introducing a first biomechanical model of aortic interface based on a peridynamical approach of the interfacial connection (Fig. 1). Elastic long-range interactions and failure criteria of the interfacial connections have been involved in the equilibrium equations and the constitutive models of the interface [2-7].

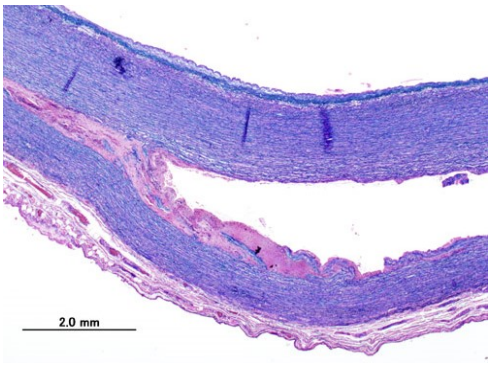

Fig. 1. Hystopatology of dissected aorta.

The numerical results obtained in the paper may be used to formulate an appropriate interface element for the biomechanical simulation of the aortic dissection.

II. Mode-I debonding and cohesive crack model

The prediction of the interfacial failure mechanisms for adhesively bonded joints and composite structures is a well-known issue that has been studied both theoretically and/or numerically [8,9]. Small loads usually leave an adhesively bonded junction, where a jump of displacements is allowed due to the compliance of the interface. An increasing load, instead, can lead to adhesive breaks in one or more interface points where a crack starts and propagates along the interface, up to the complete detachment of the adherends.

In literature, interfaces have been modeled in different ways, e.g., a narrow region of continuum with graded properties, an infinitely thin surface separated by springs, and cohesive zones with specific traction–separation relations. One of the key research issues is to determine the best way to characterize interfaces within the framework of continuum mechanics rather than using ad hoc methods only to facilitate numerical implementations, e.g. springs in finite element methods. In this context, some examples of spring layer model have been applied in [10] to capture debonding and sliding, according to a combined stress-based criterion and frictional resistance criterion. The interface models based on a continuous distribution of linear springs represent the simplest way to analyze the mechanical behavior of adhesive interfaces, (see [11-13] among others). These kinds of models are referred to as linear-elastic interfaces or weak interfaces. In this framework, the recent literature has included different stress- and energy-based parameters together with their associated failure criteria [14-18].

More recent studies, however, have successfully adopted the so called cohesive zone models (CZMs) to study the non-linear delamination, debonding, and, more generally, crack initiation and propagation within homogeneous and inhomogeneous materials and interfaces [19-21]. This is mainly related to the computational efficiency of these models and to their versatility for numerical implementations in many fields of computational mechanics. CZMs describe the traction-separation behavior of interfaces before and during fracture, and they are characterized by two phases, i.e. an increase of the traction up to a peak value and a subsequent decrease to zero, which describe the crack initiation and the growth of cohesive surfaces until new traction-free surfaces appear.

Among a large variety of test configurations, we select herein a standard specimen named double cantilever beam (DCB). This is the commonly used specimen to determine the mode-I critical energy release rate or interlaminar fracture energy of fiber-reinforced polymer composites (ISO 15024, ASTM D5528-01). For this kind of specimen, a pioneering work was provided by Kanninen [22], whereas some CZMs have been more recently developed by de Morais [23], and Dimitri et al. [24], based on a Euler-Bernoulli beam theory. In line with the last two works, the present study aims at developing a new approach to model the onset and propagation of debonding in the DCB specimen. We adopt the CZM, assuming a linear-elastic behavior for the adherends and concentrating all non-linearities at the interface. The CZM solution is found in a numerical sense for an elastic-plastic cohesive law, and an interface of finite length, while determining interfacial stresses, load-displacement curves, and critical load. In this regard, the problem of mode-I debonding of a double cantilever beam is introduced

below. The beams are modeled as Euler Bernoulli beams connected by a cohesive interface, as shown in Fig. 2.

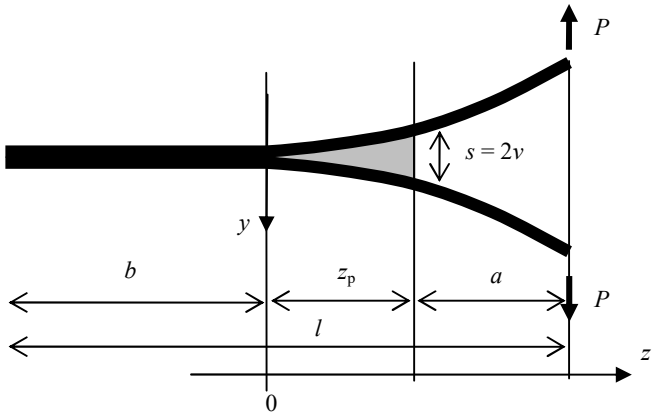

Fig. 2. Double beam model.

In Fig. 2 a is the crack length, z_p is the fracture process zone (FPZ) length, P is the applied loading and s is the relative displacement between the two beams; each beam has a thickness equal to h. In the region where $z<0$ the cohesive interface is still in the elastic region.
The governing differential equation of the problem reads as follows

$$\frac{d^4 s}{dz^4} + \frac{2t\sigma(s)}{EI} = 0 \tag{1}$$

where t is the beam depth, E and I refer to the elastic modulus and moment of inertia of the beam, respectively, and $\sigma(s)$ is the normal stress across the interface and the mechanical behavior of the interface is locally described by a cohesive stress-separation law. Typical cohesive laws applied in the literature have a trapezoidal or bilinear forms, as depicted in Fig. 3, G_{Ic} being the critical energy that dictates the fracturing process.

The interfacial laws depicted in Fig. 3 are completely defined by three parameters, namely the peak stress σ_p, the corresponding relative displacement s_p and the ultimate relative displacement s_f. To the purpose of simplifying the problem and highlighting the effect of parameters on the structural response, Eq. (1) is redefined in a dimensionless form, as already proposed in [27]. More specifically, lengths are normalized with respect to the characteristic length, as follows

$$l_{ch} = \sqrt[4]{\frac{2EI}{kt}} \tag{2}$$

where $k = \sigma_p / s_p$. The dimensionless longitudinal coordinate in the cohesive zone (namely, the FPZ) is here referred to as $\bar{z} = z / l_{ch}$, the dimensionless total length of the specimen is defined by $\bar{l} = l / l_{ch}$, whereas the dimensionless crack length and bonded length of the specimen are given by $\bar{a} = a / l_{ch}$ and $\bar{b} = b / l_{ch}$, respectively. Moreover, the dimensionless relative separation and ductility are defined as $\delta = s / s_p$ and $\mu = s_f / s_p$, respectively. Under these assumptions, the cohesive law may be written as

$$\frac{\sigma(\delta)}{\sigma_p} = f(\delta) \tag{3}$$

and the governing equation (1) can be recast in the following form

$$\frac{d^4 \delta}{d\bar{z}^4} + 4 f(\delta) = 0 \tag{4}$$

The explicit form of $f(\delta)$ depends on the cohesive model assumed in the DCB together with its elastic or cohesive zone. In [27], the explicit analytical solutions of Eq. (4) have been found for the two cohesive models depicted in Fig. 3, both for the case of beams of infinite and finite length.

A. Non-local cohesive model

In multi-layered biological tissues, such as arteries walls, collagen fibers go through different layers and contribute to the resistance of the interface to the separation between two adjacent layers; when collagen fiber are waved, they can be thought as a sewing between two adjacent layers. More specifically, if the collagen fibers are not normal to the interface, they transfer forces between non-adjacent beam elements. These long-range interactions may be modeled in a biomechanics context as non-local forces mutually exerted by non-adjacent beam element.

Following the well-established approach shown in [2-7], the non-local forces are thought as linearly dependent on the relative displacements between two non-adjacent beam elements and on the product of the two volume elements considered.
Moreover, the non-local forces are scaled through an attenuation function that decreases the entity of

the force as the distance between two volume elements increases.

Fig. 4 shows the simple mechanics behind the non-local forces mutually exerted between two non-adjacent volume elements located at $z=z_j$ and $z=\zeta_k$.

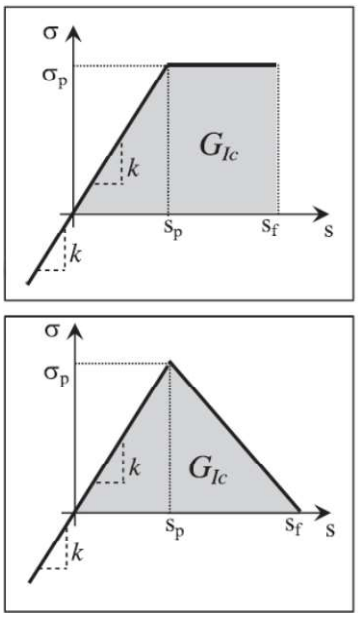

Fig. 3. Cohesive stress-separation laws, trapezoidal (up) and bilinear (down).

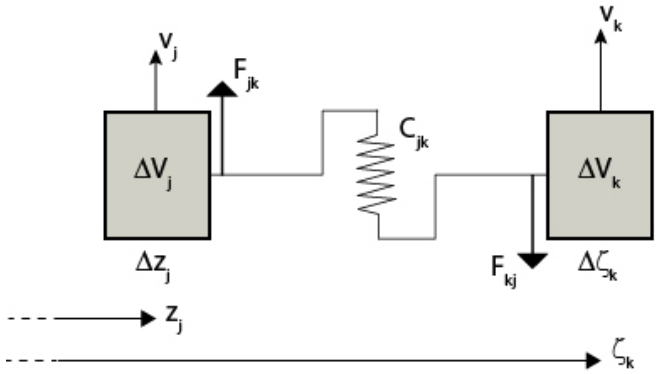

Fig. 4. Mechanics of non-local forces exchanged by two non-adjacent beam elements.

Fig. 4 shows the simple mechanics behind the non-local forces mutually exerted between two non-adjacent volume elements located at $z=z_j$ and $z=\zeta_k$. The non-local forces that the *k-th* volume element applies to the *j-th* volume element may be written as

$$F_{jk} = C_{jk}\Delta V_j \Delta V_k (s_k - s_j) \tag{5}$$

where

$$\Delta V_j = \Delta z_j th \qquad \Delta V_k = \Delta \zeta_k th \tag{6}$$

and

$$s_k = s(\zeta_k) \qquad s_j = s(z_j) \tag{7}$$

The non-local elastic coefficient C_{jk} is a variable elastic coefficient depending on the distance between the two volume elements through an attenuation function $g(\bullet)$ as follows

$$C_{jk} = C_\alpha g\left(\left|\zeta_k - z_j\right|\right) \tag{8}$$

where C_α is a parameter of the model. The resultant of all non-local forces applied to the *j-th* volume elements is evaluated as the sum of all contributions coming from all the elements of the beam as

$$F_j = C_\alpha \Delta V_j \sum_k \Delta V_k g\left(\left|\zeta_k - z_j\right|\right)(\zeta_k - s_j) \tag{9}$$

By taking the limit for $\Delta z_j, \Delta\zeta_k \to 0$ the explicit form of the resultant of non-local forces applied on the volume elements located at the generic position z is readily obtained as

$$dF(z) = C_\alpha t^2 h^2 dz \int_{-b}^{z_p} \left(s(\zeta) - s(z)\right) g\left(\left|\zeta - z\right|\right) d\zeta \tag{10}$$

Note that in Eq. (10) the integral domain is extended to the only adhesive part of the specimen, since the non-local forces do not involve the detached portion of the beams. By considering both local and non-local forces, the equilibrium equation related to the generic volume element of the beam reads

$$EI\frac{d^4 s}{dz^4} + 2t\sigma(s) + C_\alpha t^2 h^2 \int_{-b}^{z_p} \left(s(\zeta) - s(z)\right) g\left(\left|\zeta - z\right|\right) d\zeta = 0 \tag{11}$$

As far as the attenuation function is concerned, some typical laws have an exponential and power form. In this work, a power law of order α is selected as attenuation function, i.e.

$$g\left(\left|\zeta - z\right|\right) = \frac{1}{\left|\zeta - z\right|^{1+\alpha}} \tag{12}$$

By placing Eq. (12) into Eq. (11) leads to

$$EI\frac{d^4 s}{dz^4} + 2t\sigma(s) + C_\alpha t^2 h^2 \int_{-b}^{z_p} \frac{s(\zeta) - s(z)}{\left|\zeta - z\right|^{1+\alpha}} d\zeta = 0 \tag{13}$$

Eq. (13) may be written also in dimensionless form as

$$\frac{d^4 \delta}{d\bar{z}^4} + 4f(\delta) + \frac{2h^2 t}{k l_{ch}^{1+\alpha}} C_\alpha \int_{-\bar{b}}^{\bar{z}_p} \frac{\delta(\bar{\zeta}) - \delta(\bar{z})}{\left|\bar{\zeta} - \bar{z}\right|^{1+\alpha}} d\bar{\zeta} = 0 \tag{14}$$

When Eq. (14) is written in the elastic zone, it assumes the following form

$$\frac{d^4 \delta}{d\bar{z}^4} + 4\delta + \frac{2h^2 t}{k l_{ch}^{1+\alpha}} C_\alpha \int_{-\bar{b}}^{\bar{z}_p} \frac{\delta(\bar{\zeta}) - \delta(\bar{z})}{\left|\bar{\zeta} - \bar{z}\right|^{1+\alpha}} d\bar{\zeta} = 0 \tag{15}$$

whereas for the FPZ it is recast as

$$\frac{d^4\delta}{d\bar{z}^4}+4+\frac{2h^2t}{kl_{ch}^{1+\alpha}}C_\alpha\int_{-\bar{b}}^{\bar{z}_P}\frac{\delta(\bar{\zeta})-\delta(\bar{z})}{\left|\bar{\zeta}-\bar{z}\right|^{1+\alpha}}d\bar{\zeta}=0 \qquad (16)$$

In the detached zone the governing equation simply reads

$$\frac{d^4\delta}{d\bar{z}^4}=0 \qquad (17)$$

It has to be noted that Eq. (14) is an integro-differential equation, whose closed form solution is not straightforward. Hence a numerical method has been herein applied for the solution. In this regard, the central difference scheme has been adopted to perform the numerical simulations shown.

III. Numerical Simulation

In this section numerical applications are performed to investigate the non-local effects in the debonding mode-I process. For the numerical applications, the double beam element depicted in Fig. 2 is considered. The length of the beam is l=60 mm, the cross section has h=t=1 mm, and the Young modulus is $E=100$ GPa. The crack length before the application of the load is a=14 mm. The traction-separation cohesive law is described by the non-linear trapezoidal law in Fig. 3, where the selected parameters are $\sigma_P=2.5$ MPa, $s_P=0.25$ mm, and $s_f=0.75$ mm. For the non-local interaction $C_\alpha=5$ and three different values of the order α are selected, i.e., $\alpha=0.2,0.5,0.7$ to show the effect of the attenuation function in the mechanical response of the beam. In order to solve the Eq. (14), a discretization scheme is introduced and the central difference method is applied to evaluate the relation between the relative separation s(z) and the critical loading P during the mode-I debonding process. More in detail, the beam is discretized with 200 elements with a constant volume, whereby each element has the same length $\Delta z=l/n$. The matrix of the stiffness contains the local terms related to the flexural stiffness and to the non-linear interface interactions, and non-local terms, are obtained with the aid of the central difference and the discretization of the integral in Eq. (14).

Fig. 5, 6 and 7 show the deformed configuration of the beam with different values of $\alpha=0.2,0.5,0.7$ for varying values of the loading P. In Fig. 8, the load P vs separation s is shown for the three cases with non-local terms as well as in total absence of non-locality.

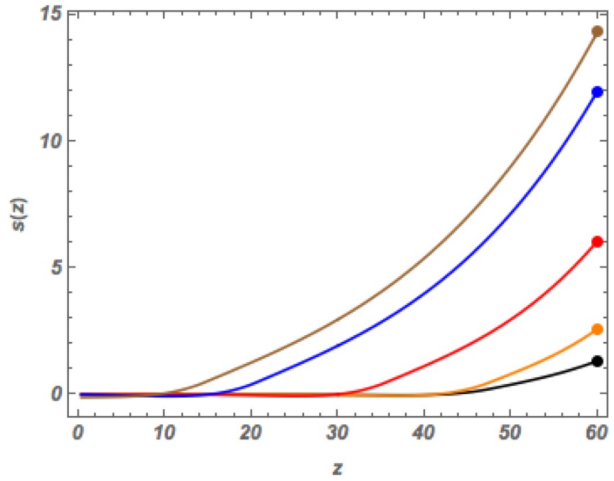

Fig. 5. Evolution of the deformed configuration of the beam for different values of the applied load P ($\alpha=0.2$).

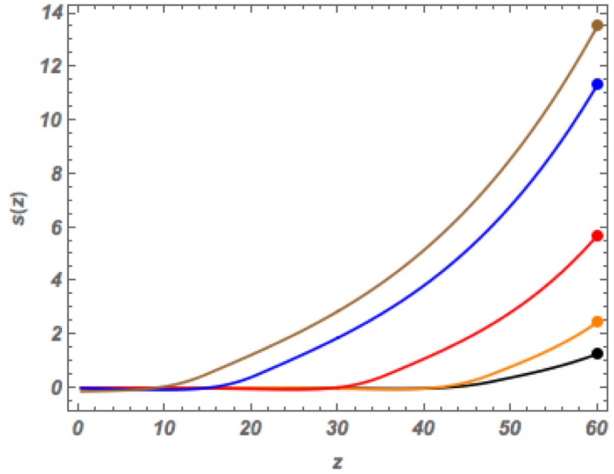

Fig. 6. Evolution of the deformed configuration of the beam for different values of the applied load P ($\alpha=0.5$).

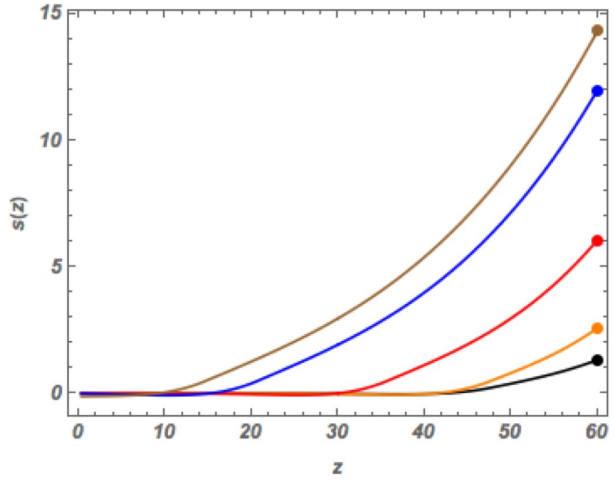

Fig. 7. Evolution of the deformed configuration of the beam for different values of the applied load P ($\alpha=0.7$).

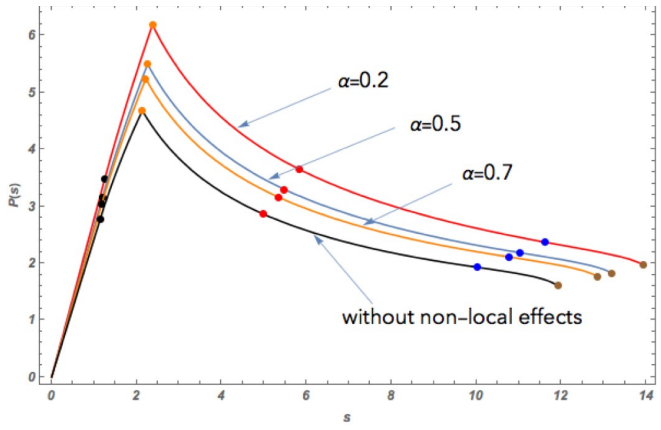

Fig. 8. Load P vs. separation s for different values of the non-local parameters.

IV. Concluding Remarks

In this work a non-local cohesive zone model has been adopted to reproduce the physical phenomenon known as arterial dissection. In the proposed model, the interface is able to transmit local elasto-plastic actions and non-local elastic long-range interactions. It is shown that the variation of non-local parameters yields to a different mechanical behavior. Such parameters must be selected accurately with the aid of experimental tests on biomechanical tissues.

Acknowledgment

R. Dimitri, F. P. Pinnola and G. Zavarise gratefully acknowledge the support received from the Italian Ministry of University and Research, through the PRIN 2015 funding scheme (project 2015JW9NJT Advanced mechanical modeling of new materials and structures for the solution of 2020 Horizon challenges).

References

[1] K. Li, R.W. Ogden, and G.A. Holzapfel, "Computational method for excluding fibers under compression in modeling soft fibrous solids" European Journal of Mechanics - A/Solids, vol. 57, pp. 178-193, 2016.

[2] M. Zingales, M. Di Paola, G. Failla. "The mechanically-based approach to 3D non-local linear elasticity theory: Long-range central interactions", International Journal of Solids and Structures, vol. 47 (18-19), pp. 2347-2358, 2010.

[3] M. Di Paola, G. Failla, A. Pirrotta, A. Sofi, M. Zingales. "The mechanically based non-local elasticity: An overview of main results and future challenges", Philosophical Transactions of the Royal Society A: Mathematical, Physical and Engineering Sciences, vol. 371(1993), 20120433, 2013.

[4] G. Alotta, G. Failla, M. Zingales. "Finite element method for a nonlocal Timoshenko beam model." Finite Element in Analysis and Design, vol. 89, pp. 77-92, 2014.

[5] G. Alotta, G. Failla, M. Zingales. "Finite element formulation of a nonlocal hereditary fractional order Timoshenko beam," Journal of Engineering Mechanics - ASCE (2017), vol 143 (5), D4015001

[6] G. Alotta, G. Failla, F.P. Pinnola, "Stochastic analysis of a non-local fractional viscoelastic bar forced by Gaussian white noise", ASCE-ASME Journal of Risk and Uncertainty in Engineering Systems, Part B: Mechanical Engineering,vol. 3(3), 030904, 2017.

[7] G. Alotta, M. Di Paola, G. Failla, F.P. Pinnola. "On the dynamics of non-local fractional viscoelastic beams under stochastic agencies". Composites Part, B, vol. 137, pp. 102-110, 2018.

[8] G.I. Barenblatt, "The formation of equilibrium cracks during brittle fracture. General ideas and hypotheses. Axially-summetric cracks," J. Appl Math. Mech., 1959, Vol. 23(3), pp. 622–636.

[9] D.S. Dugdale, "Yielding of steel sheets containing slits," J. Mech. Phys. Solids, 1960, Vol. 8, pp. 100–104.

[10] C.R. Ananth, and N. Chandra, "Numerical modeling of fiber push-out test in metallic and intermetallic matrix composites—Mechanics of the failure processes," J. Compos Mater., 1995, Vol. 29(11), pp. 1488–1514.

[11] M. Goland, and E. Reissner, "Stresses in cement joints," J. Appl. Mech. Trans. ASME 66, 1944, A17–A27.

[12] F. Erdogan, "Fracture Mechanics of Interfaces," Damage and Failure of Interfaces, 1997. Balkema Publishers: Rotterdam.

[13] Z. Hashin, "Thin interphase/imperfect interface in elasticity with application to coated fiber composites," J. Mech. Phys. Solids 2002, Vol. 50, pp. 2509–2537.

[14] S. Bennati, M. Colleluori, D. Corigliano, and PS. Valvo, "An enhanced beam-theory model of the asymmetric double cantilever beam (ADCB) test for composite laminates," Compos. Sci. Techol., 2009, Vol. 69, pp. 1735–1745.

[15] P. Cornetti, V. Mantič, and A. Carpinteri, "Finite fracture mechanics at elastic interfaces. Int. J. Solids Struct., 2012, Vol. 49, pp. 1022–1032.

[16] P.S. Valvo, "On the calculation of energy release rate and mode mixity in delaminated laminated beams," Eng. Fract. Mech., 2016, Vol. 165, pp. 114–139.

[17] R. Dimitri, F. Tornabene, and G. Zavarise, "Analytical and numerical modeling of the mixed-mode delamination process for composite moment-loaded double cantilever beams," Compos. Struct., 2018, Vol. 187, pp. 535–553.

[18] R. Dimitri, and F. Tornabene, "Numerical Study of the Mixed-Mode Delamination of Composite Specimens," Journal of Composite Sciences, 2018, accepted for publication. ID: jcs-298700.

[19] M.R. Wisnom, "Modelling discrete failures in composites with interface elements," Compos. Part A, 2010, Vol. 41, pp. 795–805.

[20] R. Dimitri, M. Trullo, L. De Lorenzis, and G. Zavarise, "A consistency assessment of coupled cohesive zone models for mixed-mode debonding problems," Fratt. Int. Strutt., 2012, Vol. 29, pp. 266–283.

[21] R. Dimitri, M. Trullo, L. De Lorenzis, and G. Zavarise, "Coupled cohesive zone models for mixed-mode fracture: a comparative study," Eng. Fract. Mech., 2015, Vol. 148, pp. 145–179 .

[22] M.F. Kanninen, "An augmented double cantilever beam model for studying crack propagation and arrest," Int. J. Fract., 1973, Vol. 9 (1), pp. 83–92.

[23] A.B. de Morais, "Mode I cohesive zone model for delamination in composite beams," Eng. Fract. Mech., 2013, Vol. 109, pp. 236–245.

[24] R. Dimitri, P. Cornetti, V. Mantič, M. Trullo, and L. De Lorenzis, "Mode-I debonding of a double cantilever beam: a comparison between cohesive crack modeling and Finite Fracture Mechanics", Int. J. Solids Struct., 2017, Vol. 124, pp. 57–72.